Letter

Glassy dynamics of the one-dimensional Mott insulator excited by a strong terahertz pulse

Kazuya Shinjo [1,2], Shigetoshi Sota [3], and Takami Tohyama [1]

[1] Department of Applied Physics, Tokyo University of Science, Tokyo 125-8585, Japan

[2] Computational Quantum Matter Research Team, RIKEN Center for Emergent Matter Science (CEMS), Wako, Saitama 351-0198, Japan

[3] Computational Materials Science Research Team, RIKEN Center for Computational Science (R-CCS), Kobe, Hyogo 650-0047, Japan

(Received 9 February 2022; revised 15 May 2022; accepted 18 July 2022; published 3 August 2022)

The elucidation of nonequilibrium states in strongly correlated systems holds the key to emergence of novel quantum phases. The nonequilibrium-induced insulator-to-metal transition is particularly interesting since it reflects the fundamental nature of competition between itinerancy and localization of the charge degrees of freedom. We investigate pulse-excited insulator-to-metal transition of the half-filled one-dimensional extended Hubbard model. Calculating the time-dependent optical conductivity with the time-dependent density-matrix renormalization group, we find that strong mono- and half-cycle pulses inducing quantum tunneling strongly suppress spectral weights contributing to the Drude weight $\sigma_{\rm D}$, even if we introduce a large number of carriers $\Delta n_{\rm d}$. This is in contrast to a metallic behavior of $\sigma_{\rm D} \propto \Delta n_{\rm d}$ induced by photon absorption and chemical doping. The strong suppression of $\sigma_{\rm D}$ in quantum tunneling is a result of the emergence of the Hilbert-space fragmentation, which makes pulse-excited states glassy.

DOI: 10.1103/PhysRevResearch.4.L032019

Introduction. The elucidation of nonequilibrium states in strongly correlated systems is of great interest since it promises to open a door to the emergence of novel quantum phases. Nonequilibrium quantum many-body states have recently been investigated not only in solids with light and electric fields [1–12] but also in trapped ions [13,14], cold atoms [15–17], and quantum circuits [18–23]. One of the most significant challenges in this field is how to preserve nonequilibrium states, such as the Floquet states [24–26], from thermalization [27–30], for which the realization of many-body localization (MBL) [31–33] may hold the key. Also, the nonequilibrium-induced insulator-to-metal transition is a fundamental issue associated with competition between itinerancy and localization of charge degrees of freedom. The photoinduced insulator-to-metal transitions [2,3,5–8] due to photon absorption have been suggested in the one-dimensional (1D) Mott insulator. Similarly, nonabsorbable terahertz photons with strong intensity have been suggested to induce a metallic state [10,11] via quantum tunneling [34–39].

Until now it has been commonly accepted that the breakdown of the Mott insulators via electric pulses leads to metallic states. However, we raise question about the validity of this understanding. To answer this question, we examine the possibility of the emergence of novel quantum phases such as glass phases with intermediate properties between itinerancy and MBL.

In this Letter, we investigate pulse-excited states of the half-filled 1D extended Hubbard model (1DEHM) using the time-dependent density-matrix renormalization group (tDMRG) [40–42]. We propose a Mott transition to glassy states induced by mono- and half-cycle terahertz pulses. If we excite the Mott insulating state via photon absorption, we obtain metallic states with large spectral weights contributing to the Drude component $\sigma_{\rm D}$. In contrast, we find that strong electric fields inducing the Zener breakdown [43] strongly suppress $\sigma_{\rm D}$, even if we introduce a large number of carriers. We consider that the emergence of the Hilbert-space fragmentation [44–53] due to high fields leads to glassy dynamics [54–59] as seen in fracton systems [60–67].

Model and method. To investigate nonequilibrium properties of the 1D Mott insulator, we use 1DEHM with a vector potential $A(t)$ defined as

$$\mathcal{H} = -t_{\rm h}\sum_{i,\sigma} B_{i,\sigma} + U\sum_{i} n_{i,\uparrow}n_{i,\downarrow} + V\sum_{i} n_i n_{i+1}, \qquad (1)$$

where $B_{i,\sigma} = e^{iA(t)}c^\dagger_{i,\sigma}c_{i+1,\sigma} + {\rm H.c.}$, $c^\dagger_{i,\sigma}$ is the creation operator of an electron with spin $\sigma(=\uparrow,\downarrow)$ at site i, and $n_i = \sum_\sigma n_{i,\sigma}$ with $n_{i,\sigma} = c^\dagger_{i,\sigma}c_{i,\sigma}$. We consider $(U,V) = (10,3)$ taking the nearest-neighbor hopping $t_{\rm h}$ to be the unit of energy ($t_{\rm h} = 1$), which describes the optical conductivity in a 1D Mott insulator ET-F_2TCNQ [68]. Spatially homogeneous electric field $E(t) = -\partial_t A(t)$ applied along the chain is incorporated via the Peierls substitution in the hopping terms [69]. Unless otherwise noted, we consider the half-filled 1DEHM with $L = 32$ sites. Note that we set the light velocity c, the elementary charge e, the Dirac constant $\hbar$, and the lattice constant to 1.

We assume that pulses have time dependence determined by $A(t) = A_{\rm pump}(t) + A_{\rm probe}(t)$ with $A_{\rm probe}(t) = A_0^{\rm pr}e^{-(t-t_0^{\rm pr})^2/[2(t_{\rm d}^{\rm pr})^2]}\cos[\Omega^{\rm pr}(t-t_0^{\rm pr})]$ for probe pulses. Unless

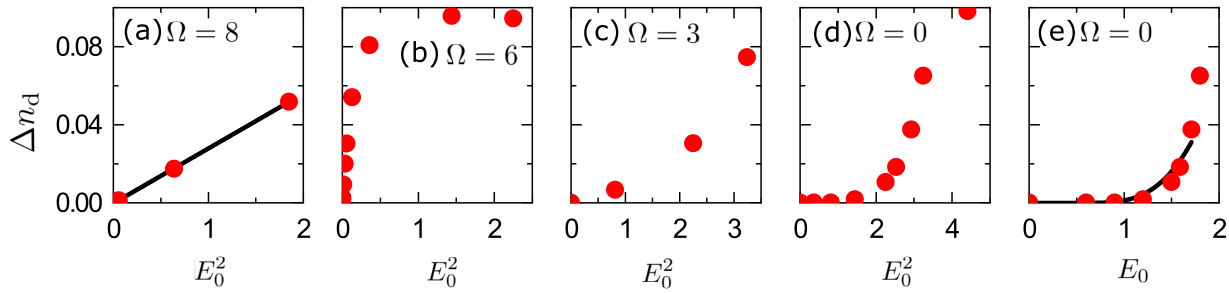

FIG. 1. $\Delta n_{\rm d}$ of the $L = 32$ half-filled 1DEHM for $(U, V) = (10, 3)$ excited by electric pulses. Red points are $\Delta n_{\rm d}$ as a function of E_0^2 for (a) $\Omega = 8$ with a black line for eye guide, (b) $\Omega = 6$, (c) $\Omega = 3$, and (d) $\Omega = 0$. (e) Red points are $\Delta n_{\rm d}$ as a function of E_0 for $\Omega = 0$. The black line shows a fitted curve proportional to $E_0 \exp(-\pi E_{\rm th}/E_0)$.

otherwise noted, we use $A_{\rm pump}(t) = A_0 e^{-(t-t_0)^2/(2t_{\rm d}^2)} \cos[\Omega(t - t_0)]$ for pump pulses. We set $A_0^{\rm pr} = 0.001$, $\Omega^{\rm pr} = 10$, $t_{\rm d}^{\rm pr} = 0.02$, and $t_0^{\rm pr} = t_0 + \tau$, where τ indicates the delay time between pump and probe pulses. We obtain time-dependent wave functions by the tDMRG implemented by the Legendre polynomical [70,71] employing open boundary conditions and keep $\chi = 3000$ density-matrix eigenstates. We obtain both singular and regular parts of the optical conductivity in nonequilibrium $\sigma(\omega, \tau) = \frac{j_{\rm probe}(\omega,\tau)}{i(\omega+i\gamma)LA_{\rm probe}(\omega)}$ [72–74], where $A_{\rm probe}(\omega)$ and $j_{\rm probe}(\omega, \tau)$ are the Fourier transform of $A_{\rm probe}(t)$ and current induced by a probe pulse, respectively (see Sec. S1 in the Supplemental Material [75]). γ indicates a broadening factor.

Doublon density. First of all, we demonstrate how pumping energy makes a difference in carrier production. Figure 1 shows how much electric pulses with $(t_{\rm d}, t_0) = (2, 10)$ change doublon density $\Delta n_{\rm d} = \frac{1}{L}[\overline{\langle I\rangle}_t - \langle I\rangle_0]$ in 1DEHM, where $I = \sum_j n_{j,\uparrow} n_{j,\downarrow}$, $\overline{\langle \mathcal{O}\rangle}_t$ is the average of an expectation value of an operator $\mathcal{O}$ from $t = 21$ to 22 just before a probe pulse is applied, and $\langle \mathcal{O}\rangle_0$ is an expectation value of $\mathcal{O}$ for a ground state. We focus on $\Delta n_{\rm d} < 0.1$, which can be achieved with experiments. $\Delta n_{\rm d}$ oscillates even after pulse decay, but their amplitudes are smaller than the radius of red points in Fig. 1. Since $\mathrm{Re}[\sigma(\omega, \tau < 0)]$ has an excitonic level at $\omega = \omega_1$ and a continuum begins at $\omega = \omega_{\rm c}$ [68,84–87], where $(\omega_1, \omega_{\rm c}) = (6, 6.5)$ for $(U, V) = (10, 3)$, a pump pulse with $\Omega = 8$ excite electrons in a continuum leading to $\Delta n_{\rm d} \propto E_0^2$ [see Fig. 1(a)] as discussed in Ref. [39] with the amplitude of electric fields E_0. Taking $\Omega = \omega_1$, we can efficiently excite doublons and holons even for small E_0 [see Fig. 1(b)]. For subgap excitations, i.e., $\Omega < \omega_1$, electrons are excited by a nonlinear process, which is classified into multiphoton absorption and quantum tunneling. The crossover between them is called the Keldysh crossover [88]. Figures 1(c) and 1(d) show $\Delta n_{\rm d}$ generated by two-photon absorption and quantum tunneling, respectively. For $\Omega = 0$ mono-cycle pulses, we find that $\Delta n_{\rm d}$ follows a threshold behavior $\Delta n_{\rm d} \propto E_0 \exp(-\pi E_{\rm th}/E_0)$ [39] as indicated by the black line in Fig. 1(e). Using this relation, we can estimate the doublon-holon correlation length $\xi \simeq \omega_1/(2E_{\rm th}) \sim 1.5$.

Glassy dynamics. We show in Fig. 2 the results of 1DEHM excited by a quantum tunneling with strong $\Omega = 0$ pulses whose energy is in terahertz band. We show $\mathrm{Re}[\sigma(\omega, \tau)]$ excited by mono-cycle pulses with $(\Omega, t_{\rm d}) = (0, 2)$ for various E_0 in Figs. 2(a)–2(c). $|E(\omega)| = |\int dt e^{i\omega t} E(t)|$ with $E_0 = 1.5$ shown in Fig. 2(d) indicates that the photon energy is too small to excite the Mott gap. We obtain $\Delta n_{\rm d} = 0.01$, 0.07, and 0.1 for Figs. 2(a)–2(c), respectively. The spectral weights above the Mott gap transfer to lower energies, but we find that the Drude weight $\sigma_{\rm D}$, which we define as spectral weight below $\omega = 0.15$ (see Secs. S2 and S3 in the Supplemental Material [75]), is not proportional to $\Delta n_{\rm d}$ but is strongly suppressed even if we take large $\Delta n_{\rm d}$ as shown in Figs. 2(b) and 2(c). Note that the Drude weight appears at

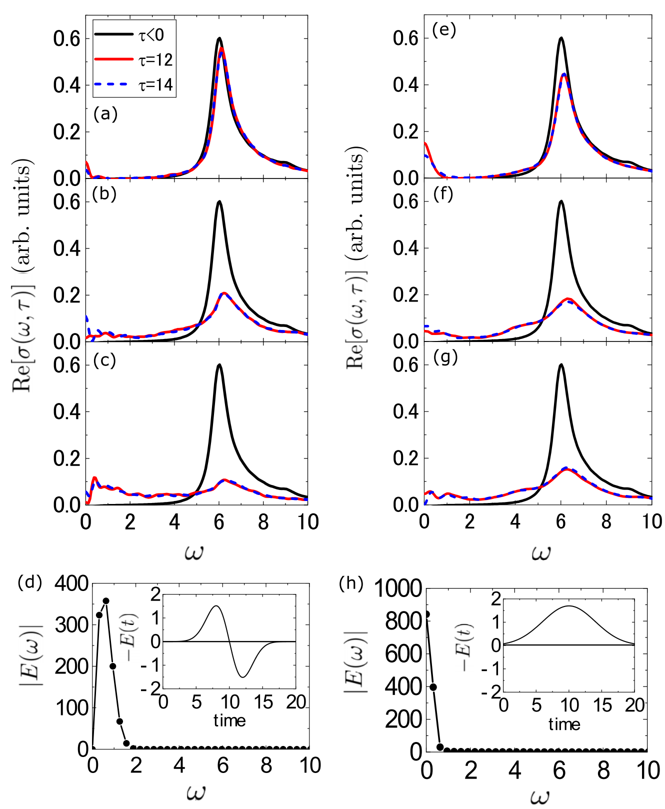

FIG. 2. $\mathrm{Re}[\sigma(\omega, \tau)]$ excited by $\Omega = 0$ mono- [half-]cycle pulses for $t_{\rm d} = 2$ [$t_{\rm d} = 4$] with (a) $E_0 = 1.5$, (b) $E_0 = 1.8$, and (c) $E_0 = 2.1$ [(e) $E_0 = 1.7$, (f) $E_0 = 1.9$, and (g) $E_0 = 2.0$]. Black, red, and blue-dashed lines are for $\tau < 0$, $\tau = 12$, and 14, respectively. (d) [(h)] $|E(\omega)|$ of a mono- [half-]cycle pulse with $E_0 = 1.5$ [$E_0 = 1.7$]. The inset indicates $-E(t)$. [(a)–(c)] and [(e)–(g)] are obtained with the half-filled $L = 32$ 1DEHM for $(U, V) = (10, 3)$ taking $\gamma = 0.4$.

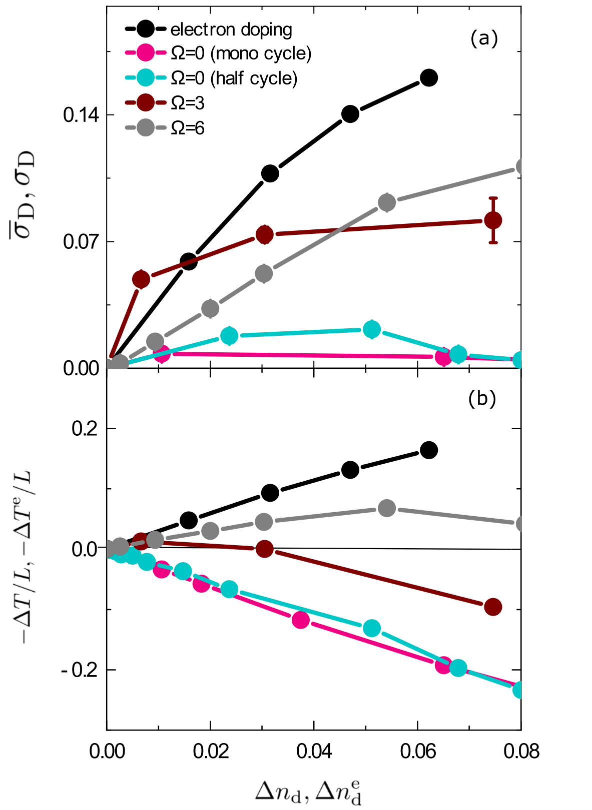

FIG. 3. (a) $\overline{\sigma}_{\mathrm{D}}$ as the function of Δn_{d} and $\Delta n_{\mathrm{d}}^{\mathrm{e}}$. $\gamma = 0.4$ is taken. (b) $-\Delta T/L$ as the function of Δn_{d} and $-\Delta T^{\mathrm{e}}/L$ as the function of $\Delta n_{\mathrm{d}}^{\mathrm{e}}$. All plots are obtained for the $L = 32$ 1DEHM.

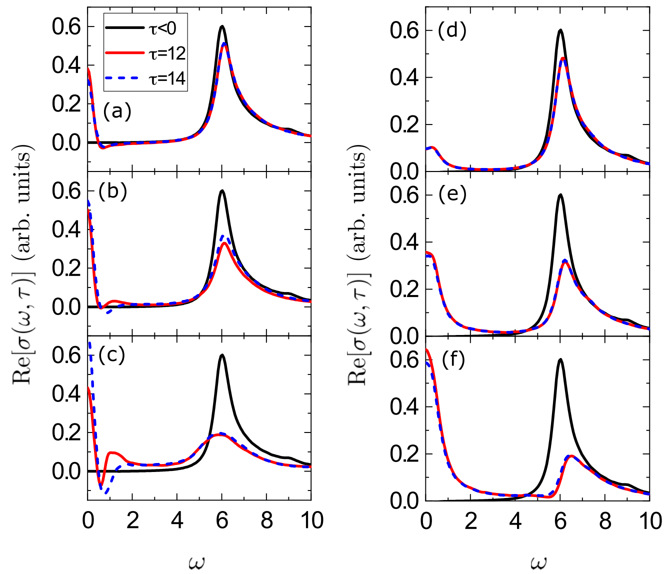

FIG. 4. $\mathrm{Re}[\sigma(\omega,\tau)]$ excited by $\Omega = 3$ [$\Omega = 6$] pulses with (a) $E_0 = 0.9$, (b) $E_0 = 1.5$, and (c) $E_0 = 1.8$ [(d) $E_0 = 0.12$, (e) $E_0 = 0.24$, and (f) $E_0 = 0.36$]. Black, red, and blue-dashed lines are for $\tau < 0$, $\tau = 12$, and 14, respectively. All plots are obtained by taking $\gamma = 0.4$ for the half-filled $L = 32$ 1DEHM with $(U, V) = (10, 3)$.

$\omega \neq 0$ due to a finite-size effect and its peak approaches $\omega = 0$ as L increases [70,89,90]. For $L = 32$, we can mask this finite-size effect by taking $\gamma = 0.4$. For half-cycle pulses, we obtain $\mathrm{Re}[\sigma(\omega,\tau)]$ as shown in Figs. 2(e)–2(g). $|E(\omega)|$ given by $E(t) = E_0 e^{-(t-t_0)^2/(2t_{\mathrm{d}}^2)} \cos[\Omega(t - t_0)]$ for $(\Omega, t_{\mathrm{d}}) = (0, 4)$ is shown in Fig. 2(h). We obtain $\Delta n_{\mathrm{d}} = 0.02$, 0.07, and 0.08 for Figs. 2(e)–2(g), respectively. Even if we find finite σ_{D} as shown in Fig. 2(e) with small Δn_{d}, further increase in Δn_{d} does not enhance σ_{D} as shown in Figs. 2(f) and 2(g), but rather suppresses it.

The strong suppression of σ_{D} suggests that strong fields localize nonequilibrium states. When a thermal state with $\sigma_{\mathrm{D}} \neq 0$ approaches an MBL state with $\sigma_{\mathrm{D}} = 0$, σ_{D} is suppressed and the center of gravity of low-energy spectral weights shifts to higher energy [91–93], which is similar to the structure seen in Figs. 2(b), 2(c), 2(f), and 2(g) when E_0 is large. The suppression of the Drude weight is clearly shown in Fig. 3(a) if we compare $\overline{\sigma}_{\mathrm{D}}$ (see below) induced by $\Omega = 0$ pulses (see magenta and light blue points) with those by photon absorption with $\Omega = 3$ (see brown points) and $\Omega = 6$ (see gray points) pulses as well as electron doping (see black points). Here, we introduce an time-averaged Drude weight $\overline{\sigma}_{\mathrm{D}} = \frac{1}{2}\sum_{\tau=12,14}\int_{\omega=0}^{2\eta} d\omega \mathrm{Re}\sigma(\omega,\tau)$ in Fig. 3(a) with $2\eta = 0.15$. Note that carrier density by electron doping are represented as $\Delta n_{\mathrm{d}}^{\mathrm{e}} = \frac{1}{2}\frac{1}{L}[\langle I\rangle_{\mathrm{doped}} - \langle I\rangle_{\mathrm{half}}]$, where $\langle \mathcal{O}\rangle_{\mathrm{doped}}$ and $\langle \mathcal{O}\rangle_{\mathrm{half}}$ are expectation values of $\mathcal{O}$ for electron-doped and half-filled 1DEHM, respectively. The factor 1/2 is introduced to compare the carrier density of electron-doped systems with that of pulse-excited systems where the same number of holons and doublons are excited. We find that σ_{D} of electron-doped 1DEHM (see Sec. S2 in the Supplemental Material [75]) has large values leading to $\sigma_{\mathrm{D}} \propto \Delta n_{\mathrm{d}}$. Upon electron doping, electrons are free to move and their kinetic energy decreases as indicated by black points in Fig. 3(b). The change of the kinetic energy for electron doped 1DEHM is defined as $\Delta T^{\mathrm{e}} = -t_{\mathrm{h}}\sum_{j,\sigma}[\langle B_{j,\sigma}\rangle_{\mathrm{doped}} - \langle B_{j,\sigma}\rangle_{\mathrm{half}}]$. Upon electron doping, spectral weights above the Mott gap transfer to those at $\omega = 0$ due to spin-charge separation [94]. Since the change of total spectral weights is determined by $-\frac{1}{2L}\Delta T^{\mathrm{e}}$ according to the optical sum rule [95], the decrease of kinetic energy contributes to the enhancement of σ_{D}. Photon absorptions also lead to metallic states following $\overline{\sigma}_{\mathrm{D}} \propto \Delta n_{\mathrm{d}}$. $\overline{\sigma}_{\mathrm{D}}$ of 1DEHM excited by $\Omega = 3$ and 6 pulses are obtained from $\mathrm{Re}[\sigma(\omega,\tau)]$, which exhibits large spectral weights at $\omega = 0$ as shown in Fig. 4. $\Omega = 3$ pulses with $E_0 = 0.9$ [Fig. 4(a)], $E_0 = 1.5$ [Fig. 4(b)], and $E_0 = 1.8$ [Fig. 4(c)] lead to $\Delta n_d = 0.007$, 0.03, and 0.07, respectively. $\Omega = 6$ pulses with $E_0 = 0.12$ [Fig. 4(d)], $E_0 = 0.24$ [Fig. 4(e)], and $E_0 = 0.36$ [Fig. 4(f)] lead to $\Delta n_d = 0.009$, 0.03, and 0.05, respectively. Note that $\overline{\sigma}_{\mathrm{D}}$ is affected by the emergence of spectral weights at $\omega \sim 0.5$ (see Sec. S3 in the Supplemental Material [75]).

In contrast to the electron-doped and photon-absorbed systems, there is no metallization when excitations are induced by a photon nonabsorbable $\Omega = 0$ pulse causing quantum tunneling. The change of kinetic energy $\Delta T = -t_{\mathrm{h}}\sum_{j,\sigma}[\overline{\langle B_{j,\sigma}\rangle_t} - \langle B_{j,\sigma}\rangle_0]$ induced by $\Omega = 0$ pulses exhibits a significant difference from other cases: $-\Delta T < 0$ monotonically decreases with increasing Δn_{d} as shown by magenta and light blue points in Fig. 3(b). We consider that a large increase in ΔT is associated with a restricted mobility due to the presence of strong fields, which leads to the strong suppression of $\overline{\sigma}_{\mathrm{D}}$.

The time evolution of an entanglement entropy $S_{\rm E} = -\sum_i p_i \ln p_i$ with the eigenvalue p_i of a reduced density matrix obtained by contracting half of the whole system shows different behavior when 1DEHM is excited by quantum tunneling and by photon absorption (see Sec. S4 in the Supplemental Material [75]). For photon absorption, $S_{\rm E}$ shows rapid linear growth and saturates at the end of pulse irradiation. On the other hand, for quantum tunneling, $S_{\rm E}$ shows slow logarithmic growth and continues to grow slowly even after the end of pulse irradiation. The slow growth of $S_{\rm E}$ [96–101] is considered to be one of the manifestations of the localized nature of excited states by a high-field terahertz pulse.

Floquet effective Hamiltonians. We see how $\Omega = 0$ pulses localize nonequilibrium states in the 1D Mott insulator. For simplicity, we consider the dc limit of the Hamiltonian (1) with $V = 0$ taking $A(t) = \Delta t$. Using the Schrieffer-Wolff transformation [24,102], we obtain an effective model for resonant driving $U = p\Delta \gg t_{\rm h}$, taking nonzero integers p. Due to the collective nature of the Zener breakdown, tunneling occurs not only between nearest-neighbor sites but also across several sites associated with $\Delta \leqslant U$ [34–39]. The $\xi \sim 1.5$ indicates that the dominant contribution to the breakdown is quantum tunneling within a few sites, which can be described as the effect of resonant electric fields with $\Delta = U/p$ for $p \lesssim 3$. The leading-order effective Hamiltonians for $p = 1, 2,$ and 3 are

$$\mathcal{H}^{(0)}_{p=1} = -t_{\rm h} \sum_{j,\sigma} (h^\dagger_{j+1j,\sigma} + h_{j+1j,\sigma}),$$

$$\mathcal{H}^{(1)}_{p=2} = \frac{t_{\rm h}^2}{\Delta}\big[(T_1 + T_1^\dagger) - 2(T_2 + T_2^\dagger) + H^a_D - T_{XY}\big] + \frac{t_{\rm h}^2}{3\Delta}\big(H^b_D - T^b_3 - T_{XY}\big),$$

$$\mathcal{H}^{(1)}_{p=3} = \frac{t_{\rm h}^2}{2\Delta}\big(H^a_D - T_{XY}\big) + \frac{t_{\rm h}^2}{4\Delta}\big(H^b_D - T^b_3 - T_{XY}\big),$$

respectively (see Sec. S5 in the Supplemental Material [75]), where

$$h^\dagger_{ji,\sigma} = n_{j,-\sigma}(1 - n_{i,-\sigma}) c^\dagger_{j,\sigma} c_{i,\sigma},$$

$$T_1 = \sum_{j,\sigma} n_{j+2,-\sigma}(1 - n_{j,-\sigma})(1 - 2n_{j+1,-\sigma}) c^\dagger_{j+2,\sigma} c_{j,\sigma},$$

$$T_2 = \sum_{j,\sigma} n_{j+2,\sigma}(1 - n_{j,-\sigma}) c^\dagger_{j+2,-\sigma} c_{j+1,-\sigma} c^\dagger_{j+1,\sigma} c_{j,\sigma},$$

$$H^a_D = \sum_{j,\sigma} n_{j+1,-\sigma}[-n_{j,\sigma} + 2n_{j+1,\sigma}(1 - n_{j,-\sigma})],$$

$$H^b_D = \sum_{j,\sigma} n_{j,\sigma}[-n_{j+1,-\sigma} + 2n_{j,-\sigma}(1 - n_{j+1,-\sigma})],$$

$$T^b_3 = \sum_{j,\sigma} n_{j,\sigma}(1 - n_{j+2,-\sigma}) \times (c_{j,-\sigma} c^\dagger_{j+1,-\sigma} c^\dagger_{j+1,\sigma} c_{j+2,\sigma} + \text{H.c.}),$$

$$T_{XY} = \sum_{j,\sigma} [(1 - n_{j,-\sigma})(1 - n_{j,\sigma}) + n_{j+1,-\sigma} n_{j+1,\sigma}] \times c^\dagger_{j,-\sigma} c_{j+1,-\sigma} c^\dagger_{j+1,\sigma} c_{j,\sigma}.$$

The effective Hamiltonians suggest that the Floquet metastable states have conservations due to $[P + I, \mathcal{H}^{(0)}_{p=1}] = [P + 2I, \mathcal{H}^{(1)}_{p=2}] = [P, \mathcal{H}^{(1)}_{p=3}] = [I, \mathcal{H}^{(1)}_{p=3}] = 0$, where $P = \sum_k k n_k$ is the dipole moment. Since the resonance condition induces real excitations, the effect of a strong electric field remains in excited states even after a pulse disappears. Such conservation may break ergodicity and lead to exotic many-body dynamics. Indeed, it has numerically demonstrated that $\mathcal{H}^{(0)}_{p=1}$ can induce ergodicity-breaking many-body eigenstates [49] like quantum many-body scarring [103–115]. Also, dynamics governed by $\mathcal{H}^{(1)}_{p=2}$ is known to be nonergodic [44]. Kinetic constraints imposed by such conservation lead to the emergent fragmentation of the Hilbert space, generating exponentially many disconnected subspaces [44–53] even within a single symmetry sector. Dipole-moment-conserved system is a representative system with such restriction as seen in fractons [60–67], which localize charge excitations topologically. T^b_3 included in $\mathcal{H}^{(1)}_{p=2}$ and $\mathcal{H}^{(1)}_{p=3}$ conserving both P and I is an example of showing doublon-assisted dipole-moment conserving processes, which does not produce Drude weight/superfluid density [116].

A strong $\Omega = 0$ pulse produce two effects in excited states: one is the injection of carriers promoting itinerancy, and the other is the restriction of motion promoting localization. As a result of their competing effects, the localization effect prevails in the $U \sim 10$ strong coupling region, and the excited states follow glassy dynamics [54–59] with weak-ergodicity breaking. We see the strong suppression of $\sigma_{\rm D}$ for $U = 7$ and 13 fixing $V/U = 0.3$ (see Sec. S6 in the Supplemental Material [75]). However, the suppression of $\sigma_{\rm D}$ for $U = 7$ is weaker than that for $U = 10$ and 13. This is because glassy states are unlikely to emerge in weak-coupling region, since the above discussion with the effective Hamiltonians is valid in strong-coupling regime. We note that the glassy state proposed in this Letter has a different origin from that induced by randomness near the Mott transition [117–122]. We expect that the glassy dynamics may be detected in ET-F_2TCNQ excited by a terahertz pulse with amplitude about 3.5 MV/cm.

Summary. We have investigated $\text{Re}[\sigma(\omega, \tau)]$ of pulse-excited states of the half-filled 1DEHM using tDMRG. We have proposed that an insulator-to-glass transition is induced by strong mono- and half-cycle pulses, which leads to the suppression of $\sigma_{\rm D}$. This is in contrast to the insulator-to-metal transition that occurs upon excitation by photon absorption accompanying $\sigma_{\rm D} \propto \Delta n_{\rm d}$. Restricted mobility due to strong fields induces glassy dynamics as seen in fracton systems. Not glassy but metallic states have been observed in the Mott insulator κ-(ET)$_2$Cu[N(CN)$_2$]Br excited by terahertz pulses in the experiment [11]. One possibility is that the enhancement of $\sigma_{\rm D}$ has been observed during electric field irradiation when nonequilibrium metastable states have not yet been reached (see Sec. S7 in the Supplemental Material [75]). Another possibility is that electron correlation is not so large that the subspaces in the fragmented Hilbert space are connected. Lastly, we note that qualitative differences in $\text{Re}[\sigma(\omega, \tau)]$ between photon absorptions and quantum tunnelings have recently been observed in a Mott insulator Ca_2RuO_4 [123].

Acknowledgments. We acknowledge discussions with H. Okamoto, K. Iwano, T. Yamaguchi, A. Takahashi, and Y. Murakami. This work was supported by CREST (Grant No. JPMJCR1661), the Japan Science and Technology Agency, by the Japan Society for the Promotion of Science, KAKENHI (Grants No. 17K14148, No. 19H01829, No. 19H05825, and No. 21H03455) from Ministry of Education, Culture, Sports, Science, and Technology (MEXT), Japan, and by JST PRESTO (Grant No. JPMJPR2013). Numerical calculation was carried out using computational resources of HOKUSAI at RIKEN Advanced Institute for Computational Science, the supercomputer system at the information initiative center, Hokkaido University, the facilities of the Supercomputer Center at Institute for Solid State Physics, the University of Tokyo, and supercomputer Fugaku provided by the RIKEN Center for Computational Science through the HPCI System Research Project (Project ID: hp170325, hp220048).

[1] G. Yu, C. H. Lee, A. J. Heeger, N. Herron, and E. M. McCarron, Transient Photoinduced Conductivity in Single Crystals of $YBa_2Cu_3O_{6.3}$: "Photodoping" to the Metallic State, Phys. Rev. Lett. **67**, 2581 (1991).

[2] Y. Taguchi, T. Matsumoto, and Y. Tokura, Dielectric breakdown of one-dimensional Mott insulators Sr_2CuO_3 and $SrCuO_2$, Phys. Rev. B **62**, 7015 (2000).

[3] S. Iwai, M. Ono, A. Maeda, H. Matsuzaki, H. Kishida, H. Okamoto, and Y. Tokura, Ultrafast Optical Switching to a Metallic State by Photoinduced Mott Transition in a Halogen-Bridged Nickel-Chain Compound, Phys. Rev. Lett. **91**, 057401 (2003).

[4] A. Cavalleri, T. Dekorsy, H. H. W. Chong, J. C. Kieffer, and R. W. Schoenlein, Evidence for a structurally-driven insulator-to-metal transition in VO_2: A view from the ultrafast timescale, Phys. Rev. B **70**, 161102(R) (2004).

[5] H. Okamoto, H. Matsuzaki, T. Wakabayashi, Y. Takahashi, and T. Hasegawa, Photoinduced Metallic State Mediated by Spin-Charge Separation in a One-Dimensional Organic Mott Insulator, Phys. Rev. Lett. **98**, 037401 (2007).

[6] K. A. Al-Hassanieh, F. A. Reboredo, A. E. Feiguin, I. González, and E. Dagotto, Excitons in the One-Dimensional Hubbard Model: A Real-Time Study, Phys. Rev. Lett. **100**, 166403 (2008).

[7] A. Takahashi, H. Itoh, and M. Aihara, Photoinduced insulator-metal transition in one-dimensional Mott insulators, Phys. Rev. B **77**, 205105 (2008).

[8] S. Wall, D. Brida, S. R. Clark, H. P. Ehrke, D. Jaksch, A. Ardavan, S. Bonora, H. Uemura, Y. Takahashi, T. Hasegawa, H. Okamoto, G. Cerullo, and A. Cavalleri, Quantum interference between charge excitation paths in a solid-state Mott insulator, Nat. Phys. **7**, 114 (2011).

[9] H. Okamoto, T. Miyagoe, K. Kobayashi, H. Uemura, H. Nishioka, H. Matsuzaki, A. Sawa, and Y. Tokura, Photoinduced transition from Mott insulator to metal in the undoped cuprates Nd_2CuO_4 and La_2CuO_4, Phys. Rev. B **83**, 125102 (2011).

[10] M. Liu, H. Y. Hwang, H. Tao, A. C. Strikwerda, K. Fan, G. R. Keiser, A. J. Sternbach, K. G. West, S. Kittiwatanakul, J. Lu *et al.*, Terahertz-field-induced insulator-to-metal transition in vanadium dioxide metamaterial, Nature (London) **487**, 345 (2012).

[11] H. Yamakawa, T. Miyamoto, T. Morimoto, T. Terashige, H. Yada, N. Kida, M. Suda, H. M. Yamamoto, R. Kato, K. Miyagawa *et al.*, Mott transition by an impulsive dielectric breakdown, Nat. Mater. **16**, 1100 (2017).

[12] S. Ishihara, Photoinduced ultrafast phenomena in correlated electron magnets, J. Phys. Soc. Jpn. **88**, 072001 (2019).

[13] R. Blatt and C. F. Roos, Quantum simulations with trapped ions, Nat. Phys. **8**, 277 (2012).

[14] C. Monroe, W. C. Campbell, L.-M. Duan, Z.-X. Gong, A. V. Gorshkov, P. W. Hess, R. Islam, K. Kim, N. M. Linke, G. Pagano, P. Richerme, C. Senko, and N. Y. Yao, Programmable quantum simulations of spin systems with trapped ions, Rev. Mod. Phys. **93**, 025001 (2021).

[15] H. Bernien, S. Schwartz, A. Keesling, H. Levine, A. Omran, H. Pichler, S. Choi, A. S. Zibrov, M. Endres, M. Greiner *et al.*, Probing many-body dynamics on a 51-atom quantum simulator, Nature (London) **551**, 579 (2017).

[16] J. Eisert, M. Friesdorf, and C. Gogolin, Quantum many-body systems out of equilibrium, Nat. Phys. **11**, 124 (2015).

[17] R. Senaratne, S. V. Rajagopal, T. Shimasaki, P. E. Dotti, K. M. Fujiwara, K. Singh, Z. A. Geiger, and D. M. Weld, Quantum simulation of ultrafast dynamics using trapped ultracold atoms, Nat. Commun. **9**, 2065 (2018).

[18] E. A. Martinez, C. A. Muschik, P. Schindler, D. Nigg, A. Erhard, M. Heyl, P. Hauke, M. Dalmonte, T. Monz, P. Zoller, and R. Blatt, Real-time dynamics of lattice gauge theories with a few-qubit quantum computer, Nature (London) **534**, 516 (2016).

[19] H. Lamm and S. Lawrence, Simulation of Nonequilibrium Dynamics on a Quantum Computer, Phys. Rev. Lett. **121**, 170501 (2018).

[20] A. Smith, M. S. Kim, F. Pollmann, and J. Knolle, Simulating quantum many-body dynamics on a current digital quantum computer, npj Quantum Inf. **5**, 106 (2019).

[21] S.-H. Lin, R. Dilip, A. G. Green, A. Smith, and F. Pollmann, Real- and imaginary-time evolution with compressed quantum circuits, PRX Quantum **2**, 010342 (2021).

[22] M. Benedetti, M. Fiorentini, and M. Lubasch, Hardware-efficient variational quantum algorithms for time evolution, Phys. Rev. Research **3**, 033083 (2021).

[23] X. Mi, M. Ippoliti, C. Quintana *et al.*, Time-crystalline eigenstate order on a quantum processor, Nature (London) **601**, 531 (2022).

[24] M. Bukov, L. D'Alessio, and A. Polkovnikov, Universal high-frequency behavior of periodically driven systems: From dynamical stabilization to floquet engineering, Adv. Phys. **64**, 139 (2015).

[25] A. Eckardt and E. Anisimovas, High-frequency approximation for periodically driven quantum systems from a Floquet-space perspective, New J. Phys. **17**, 093039 (2015).

[26] T. Oka and S. Kitamura, Floquet Engineering of Quantum Materials, Annu. Rev. Condens. Matter Phys. **10**, 387 (2019).
[27] L. D'Alessio, Y. Kafri, A. Polkovnikov, and M. Rigol, From quantum chaos and eigenstate thermalization to statistical mechanics and thermodynamics, Adv. Phys. **65**, 239 (2016).
[28] J. M. Deutsch, Quantum statistical mechanics in a closed system, Phys. Rev. A **43**, 2046 (1991).
[29] M. Srednicki, Chaos and quantum thermalization, Phys. Rev. E **50**, 888 (1994).
[30] M. Rigol, V. Dunjko, and M. Olshanii, Thermalization and its mechanism for generic isolated quantum systems, Nature (London) **452**, 854 (2008).
[31] R. Nandkishore and D. A. Huse, Many-body localization and thermalization in quantum statistical mechanics, Annu. Rev. Condens. Matter Phys. **6**, 15 (2015).
[32] E. Altman and R. Vosk, Universal dynamics and renormalization in many-body-localized systems, Annu. Rev. Condens. Matter Phys. **6**, 383 (2015).
[33] D. A. Abanin, E. Altman, I. Bloch, and M. Serbyn, Many-body localization, thermalization, and entanglement, Rev. Mod. Phys. **91**, 021001 (2019).
[34] T. Oka, R. Arita, and H. Aoki, Breakdown of a Mott Insulator: A Nonadiabatic Tunneling Mechanism, Phys. Rev. Lett. **91**, 066406 (2003).
[35] T. Oka and H. Aoki, Ground-State Decay Rate for the Zener Breakdown in Band and Mott Insulators, Phys. Rev. Lett. **95**, 137601 (2005).
[36] T. Oka and H. Aoki, in *Quantum and Semi-Classical Percolation and Breakdown in Disordered Solids*, edited by A. K. Sen, K. K. Bardhan, and B. K. Chakrabarti (Springer-Verlag, Berlin, 2008).
[37] T. Oka and H. Aoki, Dielectric breakdown in a Mott insulator: Many-body Schwinger-Landau-Zener mechanism studied with a generalized Bethe ansatz, Phys. Rev. B **81**, 033103 (2010).
[38] M. Eckstein, T. Oka, and P. Werner, Dielectric Breakdown of Mott Insulators in Dynamical Mean-Field Theory, Phys. Rev. Lett. **105**, 146404 (2010).
[39] T. Oka, Nonlinear doublon production in a Mott insulator: Landau-Dykhne method applied to an integrable model, Phys. Rev. B **86**, 075148 (2012).
[40] S. R. White, Density Matrix Formulation for Quantum Renormalization Groups, Phys. Rev. Lett. **69**, 2863 (1992).
[41] S. R. White and A. E. Feiguin, Real-Time Evolution Using the Density Matrix Renormalization Group, Phys. Rev. Lett. **93**, 076401 (2004).
[42] A. J. Daley, C. Kollath, U. Schollwöeck, and G. Vidal, Time-dependent density-matrix renormalization-group using adaptive effective Hilbert spaces, J. Stat. Mech.: Theor. Exp. (2004) P04005.
[43] C. Zener, A theory of the electrical breakdown of solid dielectrics, Proc. R. Soc. Lond. A **145**, 523 (1934).
[44] S. Scherg, T. Kohlert, P. Sala, F. Pollmann, B. H. Madhusudhana, I. Bloch, and M. Aidelsburger, Observing non-ergodicity due to kinetic constraints in tilted Fermi-Hubbard chains, Nat. Commun. **12**, 4490 (2021).
[45] P. Sala, T. Rakovszky, R. Verresen, M. Knap, and F. Pollmann, Ergodicity Breaking Arising from Hilbert Space Fragmentation in Dipole-Conserving Hamiltonians, Phys. Rev. X **10**, 011047 (2020).
[46] V. Khemani, M. Hermele, and R. Nandkishore, Localization from Hilbert space shattering: From theory to physical realizations, Phys. Rev. B **101**, 174204 (2020).
[47] T. Rakovszky, P. Sala, R. Verresen, M. Knap, and F. Pollmann, Statistical localization: From strong fragmentation to strong edge modes, Phys. Rev. B **101**, 125126 (2020).
[48] S. Moudgalya, A. Prem, R. Nandkishore, N. Regnault, and B. A. Bernevig, Thermalization and its absence within Krylov subspaces of a constrained Hamiltonian, in *Memorial Volume for Shoucheng Zhang* (World Scientific, Singapore, 2021), pp. 147–209.
[49] J.-Y. Desaules, A. Hudomal, C. J. Turner, and Z. Papić, Proposal for Realizing Quantum Scars in the Tilted 1D Fermi-Hubbard Model, Phys. Rev. Lett. **126**, 210601 (2021).
[50] L. Herviou, J. H. Bardarson, and N. Regnault, Many-body localization in a fragmented Hilbert space, Phys. Rev. B **103**, 134207 (2021).
[51] T. Kohlert, S. Scherg, P. Sala, F. Pollmann, B. H. Madlhusudhana, I. Bloch, and M. Aidelsburger, Experimental realization of fragmented models in tilted Fermi-Hubbard chains, arXiv:2106.15586.
[52] Z. Papić, Weak ergodicity breaking through the lens of quantum entanglement, arXiv:2108.03460.
[53] S. Moudgalya, B. A. Bernevig, and N. Regnault, Quantum many-body scars and hilbert space fragmentation: A review of exact results, Rep. Prog. Phys. **85**, 086501 (2022).
[54] A. Amir, Y. Oreg, and Y. Imry, Electron glass dynamics, Annu. Rev. Condens. Matter Phys. **2**, 235 (2011).
[55] S. Gopalakrishnan and R. Nandkishore, Mean-field theory of nearly many-body localized metals, Phys. Rev. B **90**, 224203 (2014).
[56] M. van Horssen, E. Levi, and J. P. Garrahan, Dynamics of many-body localization in a translation-invariant quantum glass model, Phys. Rev. B **92**, 100305 (2015).
[57] M. Pretko, Finite-temperature screening of $U(1)$ fractons, Phys. Rev. B **96**, 115102 (2017).
[58] A. Prem, J. Haah, and R. Nandkishore, Glassy quantum dynamics in translation invariant fracton models, Phys. Rev. B **95**, 155133 (2017).
[59] Z. Lan, M. van Horssen, S. Powell, and J. P. Garrahan, Quantum Slow Relaxation and Metastability due to Dynamical Constraints, Phys. Rev. Lett. **121**, 040603 (2018).
[60] M. Pretko, Subdimensional particle structure of higher rank $U(1)$ spin liquids, Phys. Rev. B **95**, 115139 (2017).
[61] M. Pretko, Higher-spin Witten effect and two-dimensional fracton phases, Phys. Rev. B **96**, 125151 (2017).
[62] M. Pretko, The fracton gauge principle, Phys. Rev. B **98**, 115134 (2018).
[63] D. J. Williamson, Z. Bi, and M. Cheng, Fractonic matter in symmetry-enriched $U(1)$ gauge theory, Phys. Rev. B **100**, 125150 (2019).
[64] J. Sous and M. Pretko, Fractons from frustration in hole-doped antiferromagnets, npj Quantum Mater. **5**, 81 (2020).
[65] J. Sous and M. Pretko, Fractons from polarons, Phys. Rev. B **102**, 214437 (2020).
[66] M. Pretko, X. Chen, and Y. You, Fracton phases of matter, Int. J. Mod. Phys. A **35**, 2030003 (2020).
[67] R. M. Nandkishore, and M. Hermele, Fractons, Annu. Rev. Condens. Matter Phys. **10**, 295 (2019).

[68] T. Yamaguchi, K. Iwano, T. Miyamoto, N. Takamura, N. Kida, Y. Takahashi, T. Hasegawa, and H. Okamoto, Excitonic optical spectra and energy structures in a one-dimensional Mott insulator demonstrated by applying a many-body Wannier functions method to a charge model, Phys. Rev. B **103**, 045124 (2021).

[69] R. Peierls, Zur Theorie des Diamagnetismus von Leitungselektronen, Z. Phys. **80**, 763 (1933).

[70] K. Shinjo, S. Sota, and T. Tohyama, Effect of phase string on single-hole dynamics in the two-leg Hubbard ladder, Phys. Rev. B **103**, 035141 (2021).

[71] K. Shinjo, Y. Tamaki, S. Sota, and T. Tohyama, Density-matrix renormalization group study of optical conductivity of the Mott insulator for two-dimensional clusters, Phys. Rev. B **104**, 205123 (2021).

[72] C. Shao, T. Tohyama, H.-G. Luo, and H. Lu, Numerical method to compute optical conductivity based on pump-probe simulations, Phys. Rev. B **93**, 195144 (2016).

[73] K. Shinjo and T. Tohyama, Ultrafast transient interference in pump-probe spectroscopy of band and Mott insulators, Phys. Rev. B **98**, 165103 (2018).

[74] J. Rincón and A. E. Feiguin, Nonequilibrium optical response of a one-dimensional Mott insulator, Phys. Rev. B **104**, 085122 (2021).

[75] See Supplemental Material at http://link.aps.org/supplemental/10.1103/PhysRevResearch.4.L032019 for time-dependent optical conductivity in the nonequilibrium state, optical conductivities in electron-doped systems, metallic states generated by photon absorption, the time evolution of entanglement entropy, effective Hamiltonians with strong couplings and fields, the interaction dependence of optical conductivities excited by a $\Omega = 0$ pulse, and the examination of pump-pulse widths in optical spectra, which includes Refs. [76–83].

[76] Y. Mizuno, K. Tsutsui, T. Tohyama, and S. Maekawa, Nonlinear optical response and spin-charge separation in one-dimensional Mott insulators, Phys. Rev. B **62**, R4769 (2000).

[77] T. Tohyama and S. Maekawa, Nonlinear optical response in Mott insulators, J. Lumin. **94-95**, 659 (2001).

[78] M. Ono, K. Miura, A. Maeda, H. Matsuzaki, H. Kishida, Y. Taguchi, Y. Tokura, M. Yamashita, and H. Okamoto, Linear and nonlinear optical properties of one-dimensional Mott insulators consisting of Ni-halogen chain and CuO-chain compounds, Phys. Rev. B **70**, 085101 (2004).

[79] H. Kishida, H. Matsuzaki, H. Okamoto, T. Manabe, M. Yamashita, Y. Taguchi, and Y. Tokura, Gigantic optical nonlinearity in one-dimensional Mott-Hubbard insulators, Nature (London) **405**, 929 (2000).

[80] H. Kishida, M. Ono, K. Miura, H. Okamoto, M. Izumi, T. Manako, M. Kawasaki, Y. Taguchi, Y. Tokura, T. Tohyama, K. Tsutsui, and S. Maekawa, Large Third-Order Optical Nonlinearity of Cu-O Chains Investigated by Third-Harmonic Generation Spectroscopy, Phys. Rev. Lett. **87**, 177401 (2001).

[81] D. Golež, M. Eckstein, and P. Werner, Dynamics of screening in photodoped Mott insulators, Phys. Rev. B **92**, 195123 (2015).

[82] S. Ohmura, A. Takahashi, K. Iwano, T. Yamaguchi, K. Shinjo, T. Tohyama, S. Sota, and H. Okamoto, Effective model of one-dimensional extended Hubbard systems: Application to linear optical spectrum calculations in large systems based on many-body Wannier functions, Phys. Rev. B **100**, 235134 (2019).

[83] D. R. Baykusheva, H. Jang, A. A. Husain, S. Lee, S. F. R. TenHuisen, P. Zhou, S. Park, H. Kim, J.-K. Kim, H.-D. Kim, M. Kim, S.-Y. Park, P. Abbamonte, B. J. Kim, G. D. Gu, Y. Wang, and M. Mitrano, Ultrafast Renormalization of the On-Site Coulomb Repulsion in a Cuprate Superconductor, Phys. Rev. X **12**, 011013 (2022).

[84] W. Stephan and K. Penc, Dynamical density-density correlations in one-dimensional Mott insulators, Phys. Rev. B **54**, R17269 (1996).

[85] F. Gebhard, K. Bott, M. Scheidler, P. Thomas, and S. W. Koch, Optical absorption of non-interacting tight-binding electrons in a Peierls-distorted chain at half band-filling, Philos. Mag. B **75**, 47 (1997).

[86] F. H. L. Essler, F. Gebhard, and E. Jeckelmann, Excitons in one-dimensional Mott insulators, Phys. Rev. B **64**, 125119 (2001).

[87] E. Jeckelmann, Optical excitations in a one-dimensional Mott insulator, Phys. Rev. B **67**, 075106 (2003).

[88] L. Keldysh, Ionization in the field of a strong electromagnetic wave, Sov. Phys. JETP **20**, 1307 (1965).

[89] H. Hashimoto and S. Ishihara, Photoinduced correlated electron dynamics in a two-leg ladder Hubbard system, Phys. Rev. B **93**, 165133 (2016).

[90] C. Shao, T. Tohyama, H.-G. Luo, and H. Lu, Photoinduced charge carrier dynamics in Hubbard two-leg ladders and chains, Phys. Rev. B **99**, 035121 (2019).

[91] O. S. Barišić and P. Prelovšek, Conductivity in a disordered one-dimensional system of interacting fermions, Phys. Rev. B **82**, 161106(R) (2010).

[92] S. Gopalakrishnan, M. Müller, V. Khemani, M. Knap, E. Demler, and D. A. Huse, Low-frequency conductivity in many-body localized systems, Phys. Rev. B **92**, 104202 (2015).

[93] R. Steinigeweg, J. Herbrych, F. Pollmann, and W. Brenig, Typicality approach to the optical conductivity in thermal and many-body localized phases, Phys. Rev. B **94**, 180401(R) (2016).

[94] M. Ogata and H. Shiba, Bethe-ansatz wave function, momentum distribution, and spin correlation in the one-dimensional strongly correlated Hubbard model, Phys. Rev. B **41**, 2326 (1990).

[95] P. F. Maldague, Optical spectrum of a Hubbard chain, Phys. Rev. B **16**, 2437 (1977).

[96] M. Žnidarič, T. Prosen, and P. Prelovšek, Many-body localization in the Heisenberg XXZ magnet in a random field, Phys. Rev. B **77**, 064426 (2008).

[97] J. H. Bardarson, F. Pollmann, and J. E. Moore, Unbounded Growth of Entanglement in Models of Many-Body Localization, Phys. Rev. Lett. **109**, 017202 (2012).

[98] M. Serbyn, Z. Papić, and D. A. Abanin, Universal Slow Growth of Entanglement in Interacting Strongly Disordered Systems, Phys. Rev. Lett. **110**, 260601 (2013).

[99] R. Vosk and E. Altman, Many-Body Localization in One Dimension as a Dynamical Renormalization Group Fixed Point, Phys. Rev. Lett. **110**, 067204 (2013).

[100] A. Nanduri, H. Kim, and D. A. Huse, Entanglement spreading in a many-body localized system, Phys. Rev. B **90**, 064201 (2014).

[101] R. Singh, J. H. Bardarson, and F. Pollmann, Signatures of the many-body localization transition in the dynamics of entanglement and bipartite fluctuations, New J. Phys. **18**, 023046 (2016).

[102] M. Bukov, M. Kolodrubetz, and A. Polkovnikov, Schrieffer-Wolff Transformation for Periodically Driven Systems: Strongly Correlated Systems with Artificial Gauge Fields, Phys. Rev. Lett. **116**, 125301 (2016).

[103] N. Shiraishi and T. Mori, Systematic Construction of Counterexamples to the Eigenstate Thermalization Hypothesis, Phys. Rev. Lett. **119**, 030601 (2017).

[104] S. Moudgalya, S. Rachel, B. A. Bernevig, and N. Regnault, Exact excited states of nonintegrable models, Phys. Rev. B **98**, 235155 (2018).

[105] S. Moudgalya, N. Regnault, and B. A. Bernevig, Entanglement of exact excited states of Affleck-Kennedy-Lieb-Tasaki models: Exact results, many-body scars, and violation of the strong eigenstate thermalization hypothesis, Phys. Rev. B **98**, 235156 (2018).

[106] T. Iadecola and M. Znidaric, Exact Localized and Ballistic Eigenstates in Disordered Chaotic Spin Ladders and the Fermi-Hubbard Model, Phys. Rev. Lett. **123**, 036403 (2019).

[107] T. Iadecola, M. Schecter, and S. Xu, Quantum many-body scars from magnon condensation, Phys. Rev. B **100**, 184312 (2019).

[108] S. Ok, K. Choo, C. Mudry, C. Castelnovo, C. Chamon, and T. Neupert, Topological many-body scar states in dimensions one, two, and three, Phys. Rev. Research **1**, 033144 (2019).

[109] C. J. Turner, A. A. Michailidis, D. Abanin, M. Serbyn, and Z. Papic, Weak ergodicity breaking from quantum many-body scars, Nat. Phys. **14**, 745 (2018).

[110] C. J. Turner, A. A. Michailidis, D. A. Abanin, M. Serbyn, and Z. Papić, Quantum scarred eigenstates in a Rydberg atom chain: Entanglement, breakdown of thermalization, and stability to perturbations, Phys. Rev. B **98**, 155134 (2018).

[111] S. Choi, C. J. Turner, H. Pichler, W. W. Ho, A. A. Michailidis, Z. Papić, M. Serbyn, M. D. Lukin, and D. A. Abanin, Emergent SU(2) Dynamics and Perfect Quantum Many-Body Scars, Phys. Rev. Lett. **122**, 220603 (2019).

[112] C.-J. Lin and O. I. Motrunich, Exact Quantum Many-Body Scar States in the Rydberg-Blockaded Atom Chain, Phys. Rev. Lett. **122**, 173401 (2019).

[113] W. W. Ho, S. Choi, H. Pichler, and M. D. Lukin, Periodic Orbits, Entanglement, and Quantum Many-Body Scars in Constrained Models: Matrix Product State Approach, Phys. Rev. Lett. **122**, 040603 (2019).

[114] J. Feldmeier, F. Pollmann, and M. Knap, Emergent Glassy Dynamics in a Quantum Dimer Model, Phys. Rev. Lett. **123**, 040601 (2019).

[115] S. Moudgalya, N. Regnault, and B. A. Bernevig, η-pairing in Hubbard models: From spectrum generating algebras to quantum many-body scars, Phys. Rev. B **102**, 085140 (2020).

[116] A. Seidel, H. Fu, D.-H. Lee, J. M. Leinaas, and J. Moore, Incompressible Quantum Liquids and New Conservation Laws, Phys. Rev. Lett. **95**, 266405 (2005).

[117] V. Dobrosavljević, D. Tanasković, and A. A. Pastor, Glassy Behavior of Electrons Near Metal-Insulator Transitions, Phys. Rev. Lett. **90**, 016402 (2003).

[118] E. Dagotto, Complexity in strongly correlated electronic systems, Science **309**, 257 (2005).

[119] E. Miranda and V. Dobrosavljević, Disorder-driven non-Fermi liquid behaviour of correlated electrons, Rep. Prog. Phys. **68**, 2337 (2005).

[120] E. C. Andrade, E. Miranda, and V. Dobrosavljević, Electronic Griffiths Phase of the $d = 2$ Mott Transition, Phys. Rev. Lett. **102**, 206403 (2009).

[121] T. Itou, E. Watanabe, S. Maegawa, A. Tajima, N. Tajima, K. Kubo, R. Kato, and K. Kanoda, Slow dynamics of electrons at a metal-Mott insulator boundary in an organic system with disorder, Sci. Adv. **3**, e1601594 (2017).

[122] R. Yamamoto, T. Furukawa, K. Miyagawa, T. Sasaki, K. Kanoda, and T. Itou, Electronic Griffiths Phase in Disordered Mott-Transition Systems, Phys. Rev. Lett. **124**, 046404 (2020).

[123] X. Li, H. Ning, O. Mehio, H. Zhao, M.-C. Lee, K. Kim, F. Nakamura, Y. Maeno, G. Cao, and D. Hsieh, Keldysh Space Control of Charge Dynamics in a Strongly Driven Mott Insulator, Phys. Rev. Lett. **128**, 187402 (2022).